Static Aeroelastic Tailoring for Oblique Wing Lateral Trim

Jonathan D. Bohlmann*
Purdue University, West Lafayette, Indiana
Clinton V. Eckstrom†
NASA Langley Research Center, Hampton, Virginia
and
Terrence A. Weisshaar‡
Purdue University, West Lafayette, Indiana

Due to its asymmetrical configuration, an oblique wing aircraft may exhibit a roll-trim imbalance. To correct this imbalance, control surfaces, such as ailerons, might be deflected or built-in twists might be added. This paper explores an alternative method of achieving oblique wing roll trim. This is the concept of applying composite tailoring to the oblique wing for lateral trim. The practical use of this concept to trim an oblique wing is demonstrated through analysis of a realistic wing by a static aeroelastic computational procedure. The computational method includes the full-potential transonic aerodynamic code FLO22 and a Ritz structural plate program that is used to model the stiffness created by symmetrical, but unbalanced, advanced composite wing skins. Analysis results indicate that asymmetric composite tailoring reduces the aileron deflection needed for roll equilibrium of the oblique wing. Furthermore, the use of aeroelastic tailoring for lateral trim can reduce control surface hinge moments and drag, resulting in performance benefits when compared to an untailored wing. At the same time, however, wing-skin stresses are greater when tailoring is used, leading to potential design tradeoffs. As such, an integrated design approach would be required to evaluate the true impact of aeroelastic tailoring on the overall performance of an oblique wing.

Introduction

THE oblique wing aircraft concept, as introduced by R. T. Jones, appears well suited to transport aircraft use as well as having air combat potential.[1,2] Two features of an oblique wing aircraft, such as that sketched in Fig. 1, are appealing. The first is a variable sweep feature that allows the plane to take off with the wing unswept. This allows for a shorter takeoff distance and more rapid climbout than that of a similar symmetrically swept-wing aircraft. In addition, pivoting the wing as a unit allows the aircraft to adjust to compressibility effects as speed increases. In particular, the low wave drag of the oblique wing at supersonic speeds makes it a candidate for an interceptor fighter or a long-range strike aircraft.

The oblique wing configuration has more than a few similarities with the X-29 forward swept-wing demonstrator aircraft. Both are unconventional attempts to achieve efficient, high-performance flight, taking maximum advantage of new technology.

Such unconventional solutions rarely come without a cost. In the case of the oblique wing, asymmetry creates a number of interesting but potentially troublesome problems. Among these problems are pitch-yaw-roll aerodynamic coupling, spanwise boundary-layer flow, and asymmetrical aeroelasticity. This paper specifically addresses the issue of the swept oblique wing aeroelasticity that creates some degree of roll imbalance.

Presented as Paper 88-2263 at the AIAA SDM Issues of the International Space Station, Williamsburg, VA, April 21-22, 1988; received Feb. 27, 1989; revision received Dec. 4, 1989.

*Currently Engineer at General Dynamics, Fort Worth, Texas. Member AIAA.

†Aerospace Engineer, Configuration Aeroelasticity Branch. Member AIAA.

‡Professor, School of Aeronautics and Astronautics. Associate Fellow AIAA.

Two previous studies have examined the effects of static aeroelasticity upon roll equilibrium of the oblique wing aircraft.[3,4] Whereas neither study considered the effect of advanced composite materials, they indicated that at high speeds some combination of asymmetrical aileron displacement and jig shape is necessary to preserve lateral trim at high dynamic pressure. The study presented here examines the use of aeroelastic tailoring, in conjunction with ailerons, for oblique wing lateral trim.

Cause of Oblique Wing Roll Imbalance

Figure 2 presents results from two analyses for subsonic flow conditions that illustrate why a swept oblique wing experiences a roll imbalance. The results are for a 30-deg swept

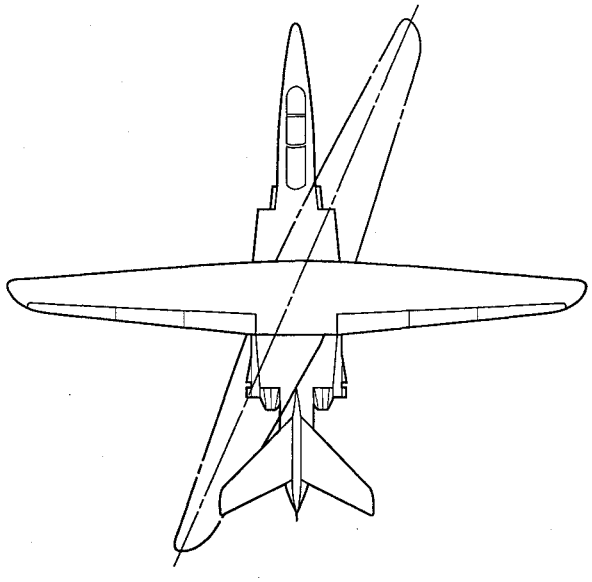

Fig. 1 Hypothetical oblique wing research aircraft.

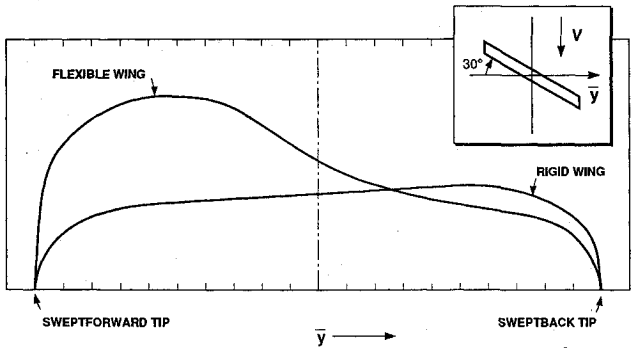

Fig. 2 Representative spanwise lift distributions for a 30-deg swept, uniform planform, oblique wing, including and excluding wing flexibility.

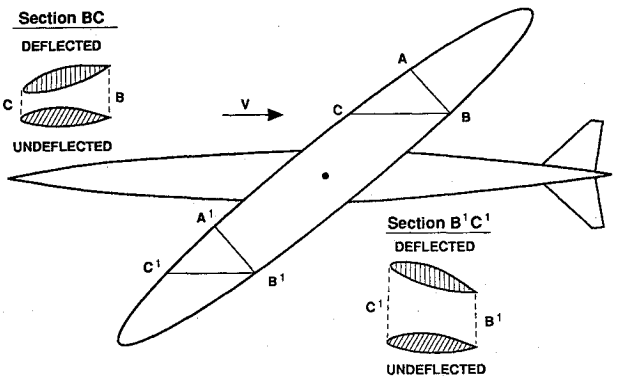

Fig. 3 Oblique wing twist due to bending.

oblique wing (no fuselage effects) restrained in roll, pitch, and plunge by clamping its root to a fixed support. In one case, the wing is assumed to be rigid, whereas in the other the analysis includes the aeroelastic effects of bending and torsional flexibility. In both cases, the initial streamwise angle of attack is the same.

The curve labeled Rigid Wing is obtained from an analysis that ignores flexibility. This curve illustrates the presence of spanwise lift asymmetry caused by spanwise inflow from the tip of the swept-forward portion toward the aft-swept wing. The result is that lift builds on the aft-swept region. This lift imbalance means that the position of the spanwise center of lift of the swept-back portion lies further outboard than the forward-swept half. Left alone, the rigid wing would thus prefer to roll with its swept-back tip moving upward while the forward-swept tip moves down. To maintain straight and level flight, a trimming roll moment must be added.

One way to reshape the spanwise lift asymmetry of the rigid wing is to alter the local streamwise angles of attack by building the wing in an initially (streamwise) distorted form. This so-called jig twist can be tailored for a specific flight condition. A second method of altering the spanwise lift distribution is to employ ailerons in such a way as to decrease outboard lift on one wing and increase it on the other. Both means have been explored in Ref. 4.

When flexibility is included, the situation is changed considerably, as Fig. 2 illustrates. Wing flexibility causes a distortion of spanwise lift that is opposite to that present for the rigid wing. The source and amount of distortion result from the phenomenon of swept-wing wash-out and wash-in due to bending.

Wash-out bending refers to the upward bending of a swept-back wing producing a reduced angle of attack when viewed from a streamwise perspective. This is depicted in Fig. 3. For a pure bending displacement, line AB on the aft-swept wing will have equal deflections. Because point C is further inboard than point B, it will have less bending displacement. This results in a decreased angle of twist due to bending, or wash-out, when viewing the wing streamwise along line CB. Similarly, bending of the forward-swept portion of the wing produces an increased streamwise angle of attack, or wash-in twist due to bending. This fundamental difference between the aerodynamic effects of bending of fore/aft-swept wings creates lift and lateral moment imbalance on oblique wings.

Aeroelastic Tailoring

Aeroelastic tailoring has been defined as "the embodiment of directional stiffness into an aircraft structural design to control aeroelastic deformation, static or dynamic, in such a fashion as to affect the aerodynamic and structural performance of the aircraft in a beneficial way."[5] The key element of this definition and the item that propels aeroelastic tailoring into prominence is the fact that lifting-surface flexibility can have a very pronounced effect on the design and success of a high-speed aircraft. In this case, distortion is both the problem and a solution to be considered in addition to jig twist and aileron actuation.

The benefits of aeroelastic tailoring may take such forms as reduced weight, increased flutter speed, greater control effectiveness, and other considerations that lead to an efficient design. Through the use of composite materials, the designer has a great deal of freedom in utilizing their high-stiffness and light-weight characteristics to tailor aeroelastic surfaces according to design goals.

The sections that follow examine the effects of aeroelastic tailoring on the lateral trim behavior of an oblique wing. A realistic oblique wing with composite wing skins is analyzed by a static aeroelastic computational procedure using FLO22 full-potential aerodynamics and a Ritz solution technique plate procedure. The performance of the tailored wing is determined by evaluating certain aerodynamic, control, and structural parameters, namely, pressure (induced) drag, required aileron deflection needed for roll trim, aileron hinge moments, and stress levels in the composite skin.

Oblique Wing Static Aeroelastic Computational Procedure

A static aeroelastic computational procedure was developed for the analysis of oblique-wing configurations.[6] This computational procedure makes use of the full-potential code FLO22[7-9] to calculate aerodynamic pressure loads and an equivalent laminated plate analysis developed by Gary Giles of NASA Langley Research Center[10,11] to calculate deflections under load for a flexible wing. FLO22 is a three-dimensional, transonic code capable of analyzing the aerodynamics of an oblique-wing configuration with no fuselage. The isentropic, steady, inviscid flow is characterized by the full-potential equation

$$(a^2-u^2)\phi_{xx}+(a^2-v^2)\phi_{yy}+(a^2-w^2)\phi_{zz}$$
$$-2uv\phi_{xy}-2uw\phi_{xz}-2vw\phi_{yz}=0$$

where ϕ is the velocity potential. The velocity is simply the derivative of the potential, its components, normalized with respect to the freestream speed, being

$$u=\phi_x, \qquad v=\phi_y, \qquad w=\phi_z$$

The three-dimensional wing is input into FLO22 by specifying the geometry at a number of chordwise stations. The geometry undergoes a series of conformal mappings and shearing transformations to define the computational domain. The reader is referred to the references cited for a detailed discussion of FLO22.

FLO22 has been previously used as part of a static aeroelastic computational procedure similar to the one devel-

oped here.[12] However, it is felt that the structural analysis procedure discussed below is an improvement over that in Ref. 12 because of its ease and effectiveness in incorporating composite materials.

The plate analysis procedure incorporates the Ritz solution technique, where the vertical deformation of the wing $W(x,y)$ is assumed to be a combination of known polynomial displacement functions $W_i(x,y)$ with unknown coefficients C_i:

$$W = C_1 W_1 + C_2 W_2 + C_3 W_3 + \ldots + C_N W_N$$

For this study, 30 displacement functions are used, corresponding to the polynomials $x^m y^n$; $m = 0$–4, $n = 2$–7. Deleting the y^0 and y^1 terms gives zero deflection and slope at the wing root.

The plate-static analysis solves the set of linear equations

$$[K]\{C_i\} = \{P_i\}$$

where $[K]$ is the equivalent stiffness matrix, C_i the displacement function coefficients, and P_i the equivalent loads, defined as

$$P_i = q \iint_{\text{area}} C_P(x,y)\, W_i(x,y)\ \text{d Area}$$

where $Cp(x,y)$ is the pressure coefficient over the planform of the wing and q the dynamic pressure. Because the pressure distribution as output by FLO22 is dependent on the wing shape and deformation in a nonlinear fashion, an iterative solution technique is required to arrive at a wing deformation that is consistent with the aerodynamic pressure loads.

Figure 4 diagrams the procedure to reach a converged shape for the flexible oblique wing under aerodynamic loads. First the FLO22 input file, which includes the three-dimensional geometric definition of the oblique wing, is developed. This geometry is then modified for the particular locations and deflections of the control surfaces given by the user. This is accomplished by a short utility program that modifies the FLO22 input file to reflect the control surfaces. The control-surface deflection does not change during an aeroelastic run. The static aeroelastic loop is then begun by the aerodynamic analysis of the wing by FLO22.

The resulting pressure distribution, which may not necessarily reflect a converged aerodynamic solution, is then converted to the equivalent loads needed by the equivalent plate program. As the wing will be treated as rigid at the midspan, and because the forward- and aft-swept halves could be structurally unsymmetric in the analysis (e.g., the forward wing given wash-out tailoring and the aft wing given wash-in tailoring), the oblique wing is split in half for the structural analysis. Thus, two sets of input are required for the plate program, as are two equivalent load vectors, one for each half of the wing. Because the pressure load is output from FLO22 as values of pressure coefficient at specific points over the wing, the equivalent loads are approximated as a finite sum, given as

$$P_k = q \sum_i \sum_j C_p(x_i,y_j) W_k(x_i,y_j) \text{Area}_{ij}$$

With the equivalent loads now known for each wing half, the equivalent plate program is invoked twice to find a separate coefficient vector $\{C_i\}$ for the fore and aft wings to define the displacement. These coefficients are input into a routine that takes the undeformed FLO22 input file and deflects the geometry for the calculated definition of the displacement. The routine determines which half of the wing it is updating and uses the appropriate set of coefficients for the displacement polynomial. The result is a FLO22 input file that reflects the deformation of the entire flexible oblique wing due to the air loads calculated from the previous shape. Note that only one FLO22 input file exists; the wing is not treated as two halves for the FLO22 analysis.

A check is now made to determine whether the deformed shape is consistent with the pressure loads used to arrive at that shape. For simplicity the convergence criterion used involves the twist of the two tips of the oblique wing structural box. If the box tip twist differs from the box tip twist of the previous iteration by a small percentage (2% is used for this analysis) for both tips, the solution is considered converged.

If convergence does not yet exist, the deformed FLO22 input file is submitted to FLO22 for aerodynamic analysis, and the aeroelastic loop is repeated until convergence is reached. A converged, deformed shape is usually achieved after three or four aeroelastic iterations. Once convergence occurs, FLO22 is entered one last time to insure that the aerodynamic pressures represent converged aerodynamic data.

Oblique-Wing Model and Analysis Procedure

The oblique-wing model used for analysis is shown in Fig. 5. An aspect ratio of 10 was chosen with a taper ratio of 0.4 and a root chord of 7.5 ft. The corresponding wing area is 275.625 ft^2. A dihedral angle of 1.25 deg is built into the wing, which helps to alleviate the load imbalance between the forward- and aft-swept sections of the wing when sweep is introduced. The airfoil section used is the supercritical airfoil OW 70-10-12, which has a 12% maximum thickness-to-chord ratio.[13]

Two outboard ailerons between the 55 and 85% semispan stations are incorporated for roll control. The hinge line is at the 70% chord line. The left and right ailerons have equal and opposite deflections δ (value of which is input and held constant for each computational run); a positive aileron deflec-

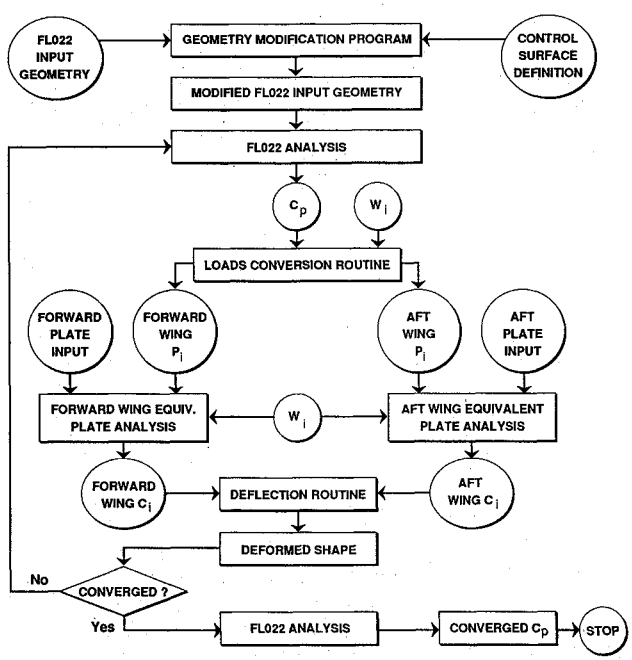

Fig. 4 Static aeroelastic computational procedure.

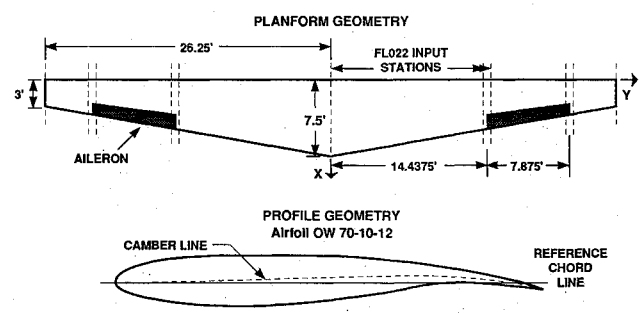

Fig. 5 Oblique wing geometry for computational model.

tion being defined as right aileron down.

The wing structural box was chosen to extend from the 10 to 70% chord lines and from midspan to 90% semispan for both halves of the wing. The depth and camber of the box are taken to be the airfoil depth and camber.

A typical graphite/epoxy material was selected for the composite material of the wing box skin, and a 0/±45/90-deg stacking sequence was used for the skin laminate (0-deg direction is parallel to the wing's leading edge). The distribution of the laminate is taken to be 60% of the skin thickness in the 0-deg direction, 15% each in the +45- and −45-deg directions, and the remaining 10% in the 90-deg orientation. This gives the predominate stiffness in the spanwise direction for this relatively high aspect ratio wing. A total skin thickness of 0.2 in. at the wing midspan was chosen with the skin thickness tapering with the airfoil thickness.

The wing was analyzed for two load conditions. Both have a wing sweep of 30 deg and a Mach number of 0.75. The "cruise condition" has a fairly typical wing loading of near 95 lb/ft^2 and corresponds to a lift coefficient of 0.44 (−0.25-deg angle of attack) and a dynamic pressure of 215 lb/ft^2. The "maneuver condition" is a 2.25 g loading condition (considering cruise as 1 g) with a lift coefficient of 0.76 (3-deg angle of attack) and a dynamic pressure of 280 lb/ft^2. The maneuver condition pressure profiles have significantly more transonic effects (stronger shock) than those for the lower angle of attack cruise condition.

The main thrust of the analysis is to examine results obtained from using various combinations of ailerons and structural tailoring to trim the oblique wing in roll. Closed-form aeroelastic solutions for the deformation of an asymmetrically swept wing have shown that structurally tailoring the wing to give a bend-up/twist-down deformation coupling (wash-out) for the forward-swept portion of the oblique wing and a bend-up/twist-up coupling (wash-in) for the aft-wing results in an aeroelastic desweeping of the wing.[6] The forward wing's wash-out tailoring alleviates, to a certain degree, its wash-in twist due to bending (discussed above), whereas the aft wing's wash-in tailoring alleviates its wash-out twist due to bending. Thus, the oblique wing with this wash-out/wash-in asymmetric tailoring behaves aeroelastically as if it had less sweep, which reduces the roll imbalance.

Adding wash-out/wash-in composite tailoring to the oblique wing is accomplished by rotating the entire skin laminate clockwise (when viewed from above). Figure 6 defines θ as the orientation angle for the rotated laminate. The fiber direction of the main composite layer is shown in the 0-deg direction for the base case of $\theta = 0$ deg.

To give the oblique wing wash-out/wash-in behavior, the laminate is rotated by the angle θ keeping the laminate continuous across the midspan. The rotation gives the forward (left) wing more directional stiffness toward the leading edge giving the desired wash-out tailoring. The aft (right) portion of the wing receives wash-in tailoring from the laminate rotation. Only one θ angle can be used per computational run.

To calculate the roll moment of the swept oblique wing about an aircraft longitudinal axis, the wing's pitching moment and rolling moment must be transformed to aircraft coordinates. This involves taking the cosine of the wing sweep times the wing's rolling moment and adding a sine contribution of the wing's pitching moment about the wing pivot. Hence, the pivot location influences the rolling moment and has a potentially large influence on the roll behavior of the wing. The pivot location of this oblique wing model is at the 22% chord point on the midspan. Combinations of aileron deflection and laminate orientation angle that give roll trim (zero rolling moment) may be determined from plots of aircraft rolling moment as functions of those two variables.

To determine advantages and disadvantages to tailoring the structure, four parameters are used as primary indicators of performance. Aerodynamic performance is measured by the pressure (induced) drag as output by FLO22. Control performance is measured by the aileron deflection needed for roll trim (less trim aileron is viewed as an advantage) and the aileron hinge moment. The hinge-moment coefficient C_H is the aileron hinge moment divided by the dynamic pressure, aileron area, and aileron mean chord. A reduced hinge moment allows reduced actuator size and less power requirements to deflect the control surface.

The wing is examined structurally to determine how tailoring affects the stresses in the wing skin. This is measured by analyzing how close the composite skin is to failing under the load. One way to determine this is by the modified Tsai-Hill criterion, given as[14]

$$f^2 = (\sigma_{11}/X)^2 + (\sigma_{22}/Y)^2 - (\sigma_{11}/X)(\sigma_{22}/X) + (\tau_{12}/S)^2$$

where σ_{11}, σ_{22}, and τ_{12} are the longitudinal, transverse, and shear stresses in the composite layer; X, Y, and S the material constants; and f the measure of the stress level in the layer. The composite layer is considered to have failed when $f^2 = 1$.

These four parameters—pressure drag, aileron deflection for roll trim, aileron hinge moment, and stress level—provide an indication of the performance tradeoffs of asymmetrically tailoring an oblique wing.

Results

Figure 7 shows combinations of aileron deflection δ and laminate orientation angle θ required to trim the oblique wing in roll. A curve of zero aircraft rolling moment is shown for both the cruise and maneuver conditions. The figure confirms that rotating the composite skin laminate to structurally wash-out the forward wing and wash-in the aft wing decreases the aileron deflection needed for lateral trim. For the cruise condition, there even exists conditions ($\theta = 13$ and 21 deg) where no aileron deflection is required to roll trim the 30-deg swept wing.

Curiously, both curves tend to flatten out and turn upward after $\theta = 15$ deg or so. This can be explained by the interplay between the wash-in and wash-out twist due to bending of the forward- and aft-swept portions of the wing, respectively, and the counteracting asymmetric tailoring being applied by the composite structure. As the composite laminate is rotated, the dominant fiber direction originally pointing out the span is moved, giving less bending stiffness.

Although this laminate rotation gives, for example, the forward wing more wash-out tailoring, the resulting decreased bending stiffness also gives the forward wing more wash-in twist due to bending. Such tradeoffs between structural tailoring and twist due to bending lead to the "bucket" phenomenon of Fig. 7. Hence, practical limits exist for the amount of asymmetric tailoring that can be effectively applied.

Figure 8 plots the pressure drag coefficient C_D vs the laminate orientation angle for the oblique wing in roll trim. An aileron deflection angle is associated with each laminate orientation angle for cruise and maneuver according to Fig. 7. For both cruise and maneuver, the pressure drag remains relatively constant as the skin laminate is rotated. This occurs because the twist distribution across the wing is basically the same for the roll-trimmed oblique wing regardless of what θ-δ combination is used to achieve that roll equilibrium. Consequently, the lift-induced drag will also change very little. It must be noted that the pressure drag as calculated by FLO22 does not include boundary-layer effects or drag from flow separation.

Referring to Fig. 7 again, a fair amount of aileron deflection is required for small laminate orientation angles, especially for the maneuver case. It is suspected that higher aileron deflections would result in a larger boundary layer and a greater likelihood of flow separation, which would result in an increase in drag not accounted for in the aerodynamic analysis of FLO22. Asymmetric tailoring could thus reduce the drag of the oblique wing because of the reduction in aileron deflection needed for roll trim.

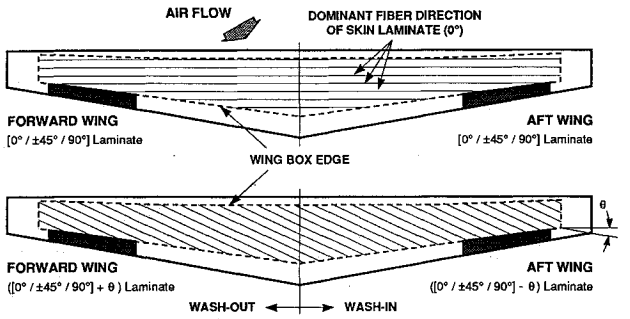

Fig. 6 Application of asymmetric tailoring to oblique wing model.

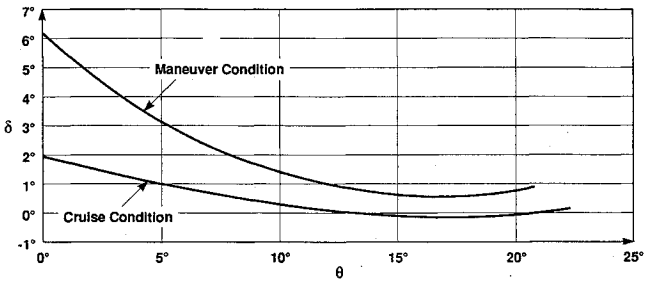

Fig. 7 Oblique wing model roll trim conditions.

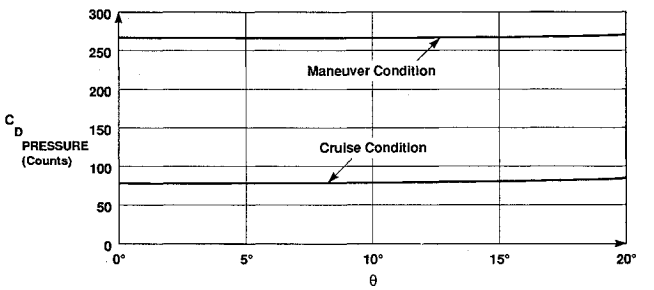

Fig. 8 Pressure drag vs laminate orientation angle for oblique wing model in roll trim.

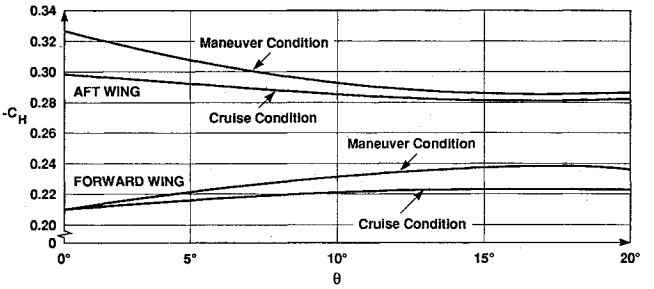

Fig. 9 Hinge moment coefficient vs laminate orientation angle for oblique wing model in roll trim.

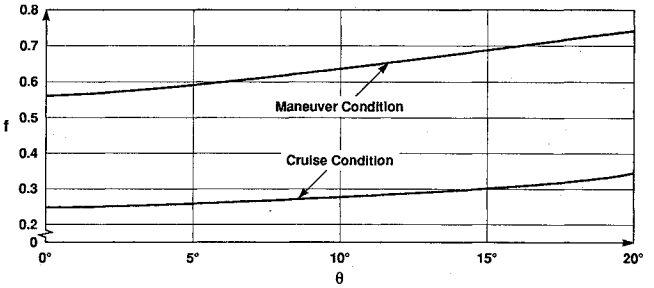

Fig. 10 Maximum skin stress level vs laminate orientation angle for oblique wing model in roll trim.

The aileron hinge moment coefficient is plotted vs laminate orientation angle in Fig. 9 for the oblique wing in roll trim. Note that considerable hinge moment exists even when the aileron is deflected less than 1 deg ($\theta \approx 15$ deg). This is due to the supercritical airfoil's large pressure toward the aft section. The hinge moment determines to a certain degree the actuator system needed for the control surfaces. Because the actuator would be the same for each aileron, consider the higher loaded aileron, which is on the aft wing. Figure 9 illustrates that for both cruise and maneuver the hinge moment is reduced due to the reduction in aileron deflection as the composite laminate is rotated.

Because of the reduced hinge moment, a smaller, lighter actuator could be used giving a weight savings. In addition, less power would be required to drive the ailerons. Aeroelastic tailoring can thus give a performance advantage by not only reduced aileron deflections but also a weight/power reduction by the resulting decrease in hinge moments.

The effect on the stress level in the composite skins due to changing the laminate orientation angle is shown in Fig. 10 for the oblique wing in roll trim. The figure depicts the maximum stress level in the composite laminate for the oblique wing. It is seen from the figure that the maximum stress level increases as the composite laminate is rotated. This is due to the laminate rotation putting the dominant fiber layer out of the spanwise direction to carry the primary bending loads. Hence, the other, less dominant layers must carry an additional load resulting in a higher stress level. This stress level increase is viewed as a disadvantage, since this would imply that the skin thickness must be increased to obtain the desired strength and factor of safety. The increase in skin thickness would cause additional weight, resulting in decreased performance.

Conclusions

Applying structural wash-out to the forward-swept portion of an oblique wing and structural wash-in to the aft-swept portion of the oblique wing has been shown, in conjunction with conventional ailerons, to provide lateral trim. The application of this asymmetric composite tailoring to a computational oblique-wing model indeed showed that less aileron deflection is needed to laterally trim such an asymmetrically tailored wing. This is due to an aeroelastic desweeping associated with the asymmetric tailoring of the wing, which counteracts the wing's inherent twist due to bending behavior. Such tailoring allows the oblique wing to maintain the aerodynamic advantages of wing sweep, while at the same time to suffer less performance penalties to trim the wing roll. This leads to a more efficient design.

The aeroelastic computational results also indicated that performance tradeoffs do exist in the application of asymmetric tailoring to the oblique wing. The decrease in the aileron requirements for roll trim leads to a reduction in aileron hinge moments. This implies a weight and power reduction since a smaller actuator could be used. The decreased aileron deflection also means that aeroelastic tailoring gives a drag reduction because of the smaller boundary layer and less likelihood of flow separation associated with less aileron deflection. However, asymmetric tailoring (at least as it was applied here) also results in an increase in the stress level in the composite wing skins. This would result in a weight increase, and hence a performance decrease, to maintain the desired strength.

Overall, it appears that a performance increase is obtained by asymmetric tailoring of an oblique wing, which leads to a more efficient and cost-effective design. Since tradeoffs exist, the use of an integrated design approach incorporating aerodynamic, structural, and control considerations would be beneficial (or necessary) for designs with aeroelastic tailoring.

Acknowledgment

This research was performed under NASA Grant NAG 1-372 at NASA Langley Research Center.

References

[1]Jones, R. T., "New Design Goals and a New Shape for the SST," *Astronautics and Aeronautics*, Vol. 10, Dec. 1972, pp. 66–70.

[2]Gregory, T. A., "Oblique Wing Ready for Research Aircraft," *Aerospace America*, Vol. 23, No. 6, 1985, pp. 78–83.

[3]Weisshaar, T. A., "Influence of Static Aeroelasticity on Oblique Wing Aircraft," *Journal of Aircraft*, Vol. 11, No. 4, 1974, pp. 247–249.

[4]Weisshaar, T. A., "Lateral Equilibrium of Asymmetrical Swept Wings: Aileron Control vs Geometric Twist," *Journal of Aircraft*, Vol. 14, No. 2, 1977, pp. 122–127.

[5]Shirk, M. H., Hertz, T. J., and Weisshaar, T. A., "Aeroelastic Tailoring—Theory, Practice, Promise," *Journal of Aircraft*, Vol. 23, No. 1, 1987, pp. 6–18.

[6]Bohlmann, J. D., "Static Aeroelasticity of a Composite Oblique Wing," M.S. Thesis, Purdue Univ., West Lafayette, Indiana, May 1987.

[7]Jameson, A., "Three Dimensional Flows Around Airfoils with Shocks," *Lecture Notes in Computer Science*, Vol. 11, Pt. 2, Springer-Verlag, Berlin, 1974, pp. 185–212.

[8]Jameson, A., "Iterative Solution of Transonic Flows over Airfoils and Wings, Including Flows at Mach 1," *Communications on Pure and Applied Mathematics*, Vol. 27, May 1974, pp. 283–309.

[9]Jameson, A., and Caughey, D. A., "Numerical Calculation of the Transonic Flow Past a Swept Wing," ERDA Mathematics and Computing Lab., New York Univ., New York, COO-3077-140, June 1977.

[10]Giles, G. L., "Equivalent Plate Analysis of Aircraft Wing Box Structures with General Planform Geometry," *Journal of Aircraft*, Vol. 23, No. 11, 1986, pp. 859–864.

[11]Giles, G. L., "Further Generalization of an Equivalent Plate Representation for Aircraft Structural Analysis," NASA TM-89105, Feb. 1987.

[12]Whitlow, W., Jr., and Bennett, R. M., "Application of a Transonic Potential Flow Code to the Static Aeroelastic Analysis of Three-Dimensional Wings," AIAA Paper 82-0689, May 1982.

[13]Kennelly, R. A., NASA-Ames Research Center, private communication, Sept. 1986.

[14]Jones, R. M., *Mechanics of Composite Materials*, McGraw-Hill, New York, 1975, pp. 76–78.